http://dx.doi.org/10.5935/0103-5053.20130188

J. Braz. Chem. Soc., Vol. 24, No. 9, 1487-1496, 2013.
Printed in Brazil - ©2013 Sociedade Brasileira de Química
0103 - 5053 $6.00+0.00

Article

The Ru–NO Bonding in Nitrosyl-[poly(1-pyrazolyl)borate]ruthenium Complexes: a Theoretical Insight based on EDA

Giovanni F. Caramori, André G. Kunitz, Daniel F. Coimbra, Leone C. Garcia and David E. P. Fonseca*

Departamento de Química, Centro de Ciências Físicas e Matemáticas, Universidade Federal de Santa Catarina, Campus Universitário Trindade, 88040-900 Florianópolis-SC, Brazil

A labilidade do grupo NO^+ em complexos $[TpRuCl_2(NO)]^q$ (Tp = BL(pirazol-1-il)$_3$) foi avaliada à luz da análise de decomposição de energia (Su-Li EDA). Os efeitos eletrônicos de diferentes substituintes pseudo-axiais (L = H, ânion pirazolato, pirazol, isoxazol e isotiazol) na natureza das ligações Ru–NO foram avaliados considerando-se os complexos no estado fundamental (GS) e nos estados meta-estáveis (MS1 e MS2). Os resultados da Su-Li EDA revelam que a natureza das ligações $\{Ru–NO\}^6$ nos complexos $[TpRuCl_2(NO)]^q$ (Tp = BL(pirazol-1-il)$_3$) é essencialmente covalente, mas apresenta ainda um caráter eletrostático significativo. A natureza dos substituintes pseudoaxiais tem um efeito direto na magnitude das ligações $\{Ru–NO\}^6$.

The lability of NO^+ group in $[TpRuCl_2(NO)]^q$ (Tp = BL(pyrazol-1-yl)$_3$) complexes was evaluated at the light of energy decomposition analysis (Su-Li EDA). The electronic effects of different pseudoaxial substituents (L = H, pyrazolyl anion, pyrazole, isoxazole and isothiazole) on the nature of Ru–NO bonding were evaluated considering complexes in ground (GS) and in metastable (MS1 and MS2) states. $\{Ru–NO\}^6$ bond nature in $[TpRuCl_2(NO)]^q$ (Tp = BL(pyrazol-1-yl)$_3$) complexes is in essence covalent, but with a still significant electrostatic character. The nature of pseudoaxial substituents has a direct effect on the magnitude of $\{Ru–NO\}^6$ bonds.

Keywords: scorpionate ligands, ruthenium nitrosyl complexes, Su-Li EDA, NBO

Introduction

Nitric oxide (NO), one of the simplest molecules in the nature, has attracted great interest from the scientific community in the last decades since it was discovered as a secretory product in mammalian cells.[1-13] NO also plays a crucial role in pathological and physiological processes[14] such as modulation of the immune and endocrine responses, blood pressure regulation,[15] neurotransmission, vasodilatation, induction of apoptosis, among others.[7,8,16] The biological effects of NO depend, in principle, on its concentration in the biological milieu. Low concentrations of NO are related with regulatory effects, while higher concentrations of nitric oxide are related with nitrosative and oxidative stress.[17]

The development of storage-release systems capable of delivering NO to desired targets has stimulated the synthesis of new transition metal compounds containing NO.[14,18-22] In this scenario, ruthenium complexes, including nitrosyl or nitrite complexes, are in the spotlight since they can not only scavenge but also release nitric oxide in a controlled way, regulating the NO-level *in vivo*.[14,21,23-47] Particularly, ruthenium(II) tetraammine nitrosyl complexes such as *trans*-$[Ru^{II}(NH_3)_4(L)NO]^{3+}$ exhibit important properties such as solubility, high stability in aqueous solutions and capability of releasing NO^0 through photochemical or chemical monoelectronic reduction.[48-51] For instance, *trans*-$[Ru^{II}(P(OEt)_3)(NO)(NH_3)_4](PF_6)_3$ can be reduced by a redox potential of –0.10 V (*vs.* SCE.), releasing NO with k_{NO} = 0.97 s^{-1} with the formation of the *trans*-$[Ru^{II}(P(OEt)_3)(H_2O)(NH_3)_4]^{2+}$ species.[48] The $\{Ru–NO\}^{6/7}$ redox potential and k_{-NO} of the tetraammine nitrosyl complexes such as *trans*-$[Ru^{II}(L)(NO)(NH_3)_4]^{q+}$ L = $Cl^–$, isonicotinamide (isn), pyridine (py), H_2O, pyrazine (pz), triethylphosphite ($P(OEt)_3$), 4-picoline (4-pic), 4-chloropyridine(4-Clpy), imidazole (im*C* or im*N*), 4-acethylpyridine (4-acpy) and L-histidine (L-hist)) can be tuned by the careful choice of the *trans* ligand L.[14,30-42] Our group addressed this issue theoretically in our previous

*e-mail: giovanni.caramori@ufsc.br

studies,[52-54] in which the influence of different ligands (tetraammines or polyamines such as cyclam, cyclen) on {Ru–NO}$^{6/7}$ bonding situation was investigated at the light of the energy decomposition analysis (EDA). Theoretical approaches, in particular electronic structure calculations rooted on quantum mechanics, enable us to shed light on the physical and chemical properties of different compounds, even before the real synthesis.[55]

In a seminal work, Onishi[56] presented the synthesis and discussed the spectroscopic properties of a new class of ruthenium nitrosyl complexes, the nitrosyl-[poly(1-pyrazolyl)borate]ruthenium(II) complexes. The importance and utility of polypyrazolyl borate ligands (also known as scorpionates) have been demonstrated by the diversity of synthesized transition-metal complexes containing such ligands.[56-64] The term scorpionate, coined by Trofimenko,[57-59] refers to a special class of tridentate ligands, in which two donor sites bind to the metal as a claw, and a third donor site binds to the metal as a sting of a scorpion, imprisoning it.[57,58] Trispyrazolylborate (Tp) is therefore highlighted as the most popular ligand of this class.[57] The tripodal coordination mode conferred by polypyrazolyl borate ligands has been shown to allow a good bonding stabilization with the metal centre due to the strong sigma bonds formed between the nitrogen and the imprisoned metal.[57-59]

After the first synthesis of nitrosyl-[poly(1-pyrazolyl) borate]ruthenium(II) complexes, [TpRuCl$_2$(NO)] (Tp = BH(pyrazol-1-yl)$_3$) (**1**),[56] different applications for this class of complexes have been achieved.[60-65] For instance, Arikawa *et al.*[60] have employed [TpRuCl$_2$(NO)] as starting material to synthesize monoacetylide complexes, which not only have a key role as intermediates in catalytic process, but also can yield ketonyl and acyl derivatives under hydration reaction.[60] Arikawa *et al.*[61] has also communicated that [TpRuCl$_2$(NO)] {Ru–NO}^{6} in presence of equimolar amount of pyrazole and excess of Et$_3$N in refluxing CH$_2$Cl$_2$ gives rise to a binuclear complex (TpRu)$_2$(μ-Cl)(μ-pz){μ-k^2-N(=O) N(=O)}, in which an easy cleaved and reversible N–N coupling between two nitrosyl ligands was observed.[61] The transformation of the above mentioned N–N coupled complex into the oxo-bridged binuclear complex with the evolution of N$_2$O was also observed, providing significant information about the mechanism of NO reduction to N$_2$O by NO reductases (NOR).[61]

It is common sense that the nature of pseudoaxial substituents and the introduction of substituents on pyrazolyl can significantly affect the chemical reactivity, as well as different properties of their transition metal complexes.[56-59] Another important aspect that should be taken into account in ruthenium nitrosyl complexes is the fact that they present photoinduced metastable states,[66,67] which are linkage isomers wherein the nitrosyl is bound through the oxygen atom (MS1) or sideways (η^2) through both nitrogen and oxygen atoms (MS2), as highlighted in Figure 1. Photoinduced metastable states were reported in 1977 by the first time, in a Mössbauer spectroscopic study of sodium nitroprusside dihydrate (SNP).[68,69] The metastable states of SNP were later confirmed by differential scanning calorimetry (DSC).[70] The ruthenium nitrosyl complexes, for which long-lived metastable states were observed,[71-75] include K$_2$[RuCl$_5$NO], [Ru(NO$_2$)$_4$(OH)NO]$^{2-}$, [Ru(CN)$_5$NO]$^{2-}$, [Ru(py)$_4$Cl(NO)](PF$_6$)$_2$·0.5H$_2$O and others. Metastable states are populated when samples are irradiated at low temperature with light of appropriate wavelength, and they are deactivated to the stable ground state isomer by red de-excitation or by thermal decay.[76,77]

In order to contribute to the comprehension of Ru–NO bonding in different classes of ruthenium nitrosyl complexes, the present work intents to shed light into the {Ru–NO}^{6} bonding situation in nitrosyl-[poly(1-pyrazolyl) borate]ruthenium(II) complexes, [TpRuCl$_2$(NO)]

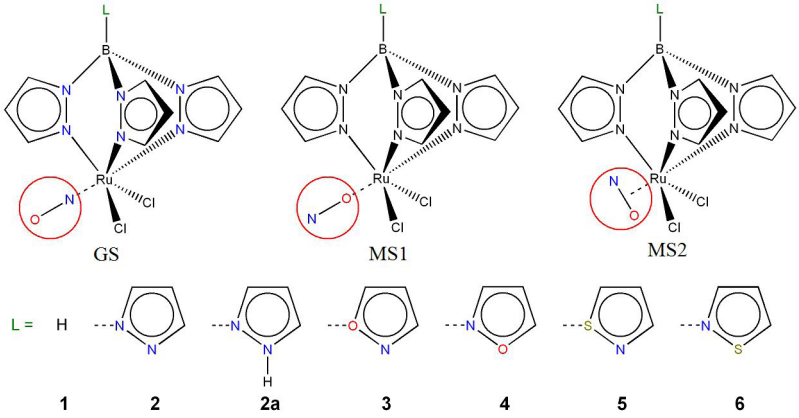

Figure 1. Schematic representation of the studied [TpRuCl$_2$(NO)] complexes, in which not only the pseudoaxial substituents, L, but also the considered states of {Ru–NO}^{6} core (ground state (GS), and photoinduced metastable states (MS1 and MS2)) are highlighted.

(Tp = BL(pyrazol-1-yl)$_3$) (**1**-**6**), by considering them not only in GS, but also in the MS1 and MS2 states, and by verifying the real dependence of the pseudoaxial substituents (L), in particular, pyrazolyl, pyrazole, isoxazole and isothiazole in different bonding situations (Figure 1). The choice of pseudoaxial ligands is rooted on the differentiation of the electronic effects of homoscorpionate (**2**) from heteroscorpionates (**1**, **2a**-**6**) ligands on the lability of {Ru–NO}^{6} bonding. For that reason, L = H (the reference for heteroscorpionates), and 1,2-azoles, comprising pyrazole, isoxazole and isothiazole. The restriction to the 1,2-azoles family is motivated by the versatility of these compounds in supramolecular chemistry and by their distinguished importance in the design and synthesis of novel biologically active compounds.[78,79]

Methodology

Geometry optimizations, harmonic frequencies and NBO analysis of complexes **1**-**6** (Figure 1) were calculated at the nonlocal DFT (density functional theory) level of theory,[80,81] by using the exchange functional of Becke[82] and the correlation functional of Perdew[83] (BP86). Ahlrichs' triple-ζ-quality basis sets (TZVP)[84,85] and scalar relativistic effects were considered for ruthenium by using the zero-order regular approximation (ZORA).[86-88] All geometry optimizations were performed employing the ORCA package.[89,90] Vibrational frequencies and NBO analysis were performed at BP86/TZVP level of theory, by using Gaussian03 package.[91]

The energy decomposition analysis developed by Su and Li[92] (Su-Li EDA) was carried out by using Zhao-Truhlar hybrid functional M06[93,94] and Ahlrichs def2-TVZP[95] and def2-SVP[96] basis sets. Su-Li EDA calculations were carried out with the GAMESS-US quantum chemistry package.[97,98] The Su-Li EDA approach[92] is rooted in the prototypical EDA methods of Kitaura and Morokuma[99-101] (KM), Ziegler and Rauk[102] (ZR) and Hayes and Stone[103] (HS) but it includes modifications and extensions of the previous ones. The Su-Li EDA approach is also feasible enough to study not only covalent bonds, but also internal rotation barriers, interaction energies in molecular clusters, nonbonding interactions, metal-ligand interactions and ionic bonds.

The EDA is focused in instantaneous interactions between fragments (*A*) of the molecule (*X*), which is the energy difference between the molecule and its fragments ($\Delta E_{int HF}$) in the frozen geometry of the compound. For a set of orthonormal molecular Hartree-Fock (HF) spin orbitals, the E^{HF} can be written in terms of orbital energy integrals, equation 1, in which *i* and *j* run over occupied spin orbitals and the one-electron and two-electron Coulomb and exchange integrals are given by h_i, $\langle ii \mid jj \rangle$ and $\langle ij \mid ij \rangle$, respectively. E^{nuc} represents the nuclear repulsion energy. For a molecule *X* constituted by *A* fragments, the total HF interaction energy ($\Delta E_{int HF}$) can be written as equation 2, in which $|\Phi_X\rangle$ and $|\Phi_A\rangle$ represent the single-determinant wavefunctions for the molecule and fragment, respectively.

$$E^{HF} = \sum_i^{\alpha,\beta} h_i + \frac{1}{2}\sum_i^{\alpha,\beta}\sum_j^{\alpha,\beta}\langle ii|jj\rangle - \frac{1}{2}\sum_i^{\alpha}\sum_j^{\alpha}\langle ij|ij\rangle - \frac{1}{2}\sum_i^{\beta}\sum_j^{\beta}\langle ij|ij\rangle + E^{nuc} \quad (1)$$

$$\Delta E_{int\,HF} = \langle \Phi_X \mid H_X \mid \Phi_X \rangle - \sum_A \langle \Phi_A \mid H_A \mid \Phi_A \rangle \quad (2)$$

According to Su-Li EDA approach,[92] $\Delta E_{int HF}$ can be decomposed into different terms, electrostatic, exchange, repulsion and polarization, equation 3. The electrostatic, repulsion and exchange terms are isolated according to the HS method.[103] Since this is based on spin orbitals, it can treat both closed and open-shell systems described by RHF, ROHF or UHF wave functions.

$$\Delta E_{int\,HF} = \Delta E^{ele} + \Delta E^{ex} + \Delta E^{rep} + \Delta E^{pol} \quad (3)$$

$$\Delta E^{disp} = \Delta E^{CCSD(T)} - \Delta E^{HF} \quad (4)$$

The polarization term is defined as the relaxation energy on going from monomers to the supermolecular orbitals. Dispersion energy (equation 4) is derived through correlation methods such as MP2 or CCSD(T). A DFT version of Su-Li EDA was also implemented in GAMESS-US package,[97,98] and in this case, the total interaction energy (ΔE^{KS}) is decomposed into electrostatic (ΔE^{ele}), exchange (ΔE^{ex}), repulsion (ΔE^{rep}), polarization (ΔE^{pol}) and dispersion (ΔE^{disp}) terms (equation 5), depending on the employed exchange and correlation functionals. Further details can be found in the Su and Li[92] work. The Boys and Bernardi[104] counterpoise method was also implemented in the Su-Li EDA approach for correcting basis set superposition error (BSSE). The polarization and dispersion terms can be gathered together, yielding the orbital term (equation 6), while the repulsion and exchange can also be combined into the Pauli repulsion component (equation 7). All 2D structures, as depicted in Figure 1, were drawn with Bkchem software.[105] Chemcraft 1.6 graphical program was employed to visualize computed results such as optimized geometries, natural orbitals and vibrational modes.[106]

$$\Delta E_{int\,KS} = \Delta E^{ele} + \Delta E^{ex} + \Delta E^{rep} + \Delta E^{pol} + \Delta E^{disp} \quad (5)$$

$$\Delta E^{orb} = \Delta E^{pol} + \Delta E^{disp} \quad (6)$$

$$\Delta E^{Pauli} = \Delta E^{ex} + \Delta E^{rep} \quad (7)$$

Results and Discussion

Ground and light-induced metastable structures

The Ru–NO bonding situation in nitrosyl-[poly(1-pyrazolyl)borate]ruthenium(II) complexes $[TpRuCl_2(NO)]^q$ (Tp = BL(pyrazol-1-yl)$_3$, L= H, pyrazolyl, pyrazole, isoxazole and isothiazole) **1**-**6**, was evaluated prior to the {Ru–NO}^{6} core reduction, considering the ground and the metastable states (Figure 2). Geometry optimization results for **1**-**2** (Table S1 in the Supplementary Information (SI) section) show that the optimized structures reproduce fairly well the available stretching frequencies of N–O and B–H bonds.[56] According to Figure 2, the structures of **1** in GS or MS1 states exhibit a pseudo-octahedral arrangement of ligands around the metallic centre, in which Ru–N–O and Ru–O–N angles are close to 180°, indicating the nitrosonium character of NO ligand.

In general, the presence of different pseudoaxial substituents does not affect considerably the metal-ligand Ru–NO bond lengths in complexes **1**-**6** (Table S1 in the SI section, Figure 3). On the other hand, the NO bond lengths (R(N–O)) are quite similar, but slightly larger for MS1 and MS2 than for GS, in agreement with the NO stretching frequencies (Table S1 in the SI section, Figure 3).

Regarding the ν(NO) stretching frequency values, they are slightly larger in **2a** than in **2**, despite the very similar NO bond lengths (Table S1 in the SI section). It can be easily explained by the inspection of the plots of the electrostatic potentials and dipole moments (Figure S1, in

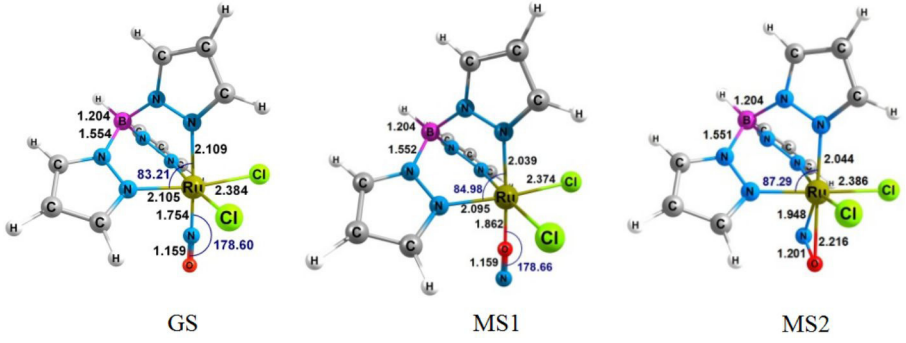

Figure 2. Optimized structures of complex **1** in the ground (GS), and metastable (MS1 and MS2) states at BP86/TZVP level of theory.

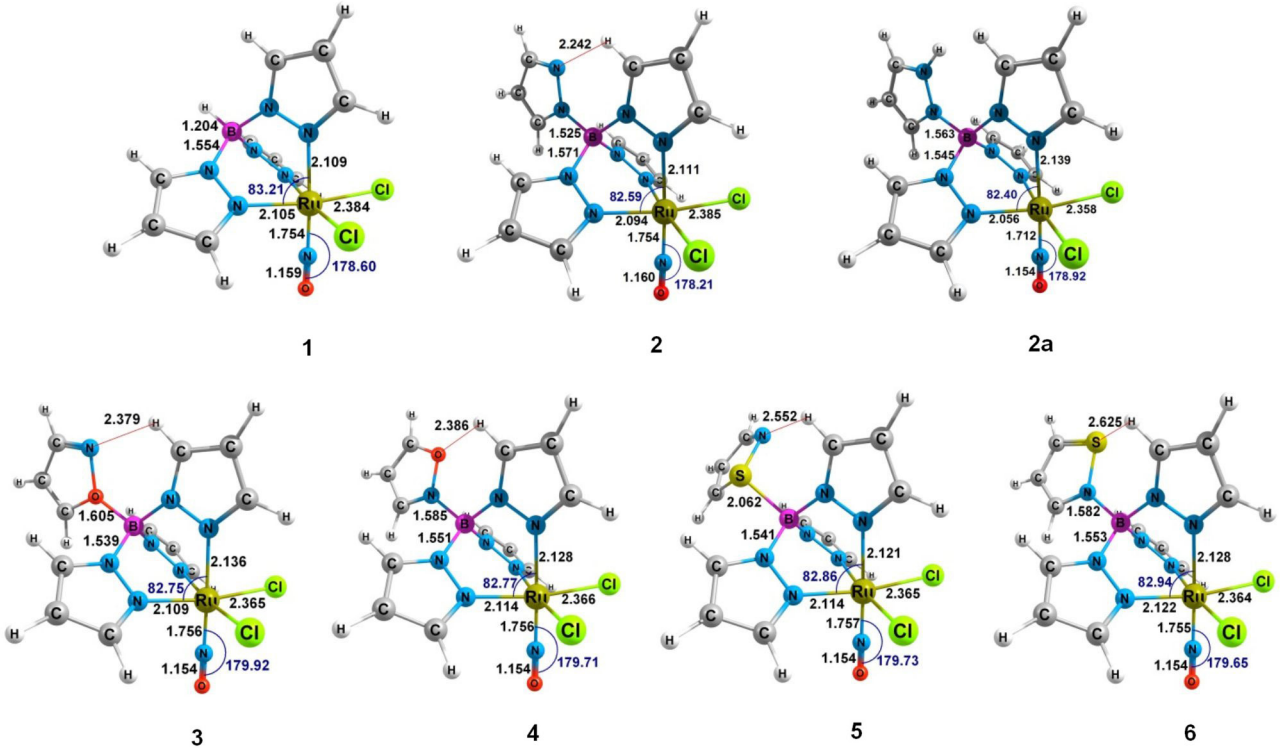

Figure 3. Optimized structures of $[TpRuCl_2(NO)]^q$ (Tp = BL(pyrazol-1-yl)$_3$, L = H, pyrazolyl anion, pyrazole, isoxazole, and isothiazole) complexes **1**-**6** in the ground state, GS, at BP86/TZVP level of theory.

the SI section). It shows that by changing the pseudo-axial ligand from pyrazolyl to pyrazole, the electron density distribution in the whole molecule changes considerably, in particular around the {Ru–NO}^{6} core. These changes can be attributed to the charge difference between pyrazolyl and pyrazole ligands, and also to the presence of a week intramolecular hydrogen bond between the pyrazolyl rings in **2** (Figure S1a in the SI section). In this case, by changing the pseudoaxial ligand from pyrazolyl (**2**) to pyrazole (**2a**), not only the magnitude but also the orientation of the dipole moment change significantly (Figure S1b in the SI section).

It is well known that in nitrosyl complexes, the infrared NO stretching band between 1950-1880 cm^{-1} is associated with the linear structure of Ru–N–O and the nitrosonium character (NO$^+$). According to Enemark and Feltham[107] canonical structures, the {Ru–NO}^{6} core, in which the total number of electrons in the metal (d) and in the nitrosyl (π^*) orbitals is indicated, is often represented by the resonance form Ru^{II}(NO$^+$), despite the fact that it is just one among several other resonance forms such as Ru^{III}(NO) and Ru^{IV}(NO$^-$). Nonetheless, the Wiberg bond order results (Table 1) reveal not only that for nitrosyl-[poly(1-pyrazolyl) borate]ruthenium(II) complexes ([TpRuCl$_2$(NO)]^q) the first resonance structure (Ru^{II}(NO$^+$)) predominates but also that it can be slightly influenced by the nature of the employed pseudoaxial ligand.

According to Table 1, on going from **1** to **6**, the double bond character of N–O bond increases in GS and in MS1. On the other hand, for MS2, the double bond character increases going from **1** to **4**, but decreases from **5** to **6**. The results also predict that for a same pseudoaxial ligand, for instance L = isoxazole, complexes **3** and **4**, the NO bond orders are affected by the bonding mode of pseudoaxial ligands. For instance, when isoxazole is bound to boron by nitrogen atom, **3**, the Ru–NO bond orders are smaller than when it is bound by oxygen atom, **4** (Table 1).

Table 1. Calculated Wiberg bond order indices, at BP86/TZVP level of theory

	GS						
	1	**2**	**2a**	**3**	**4**	**5**	**6**
N–O	1.913	1.923	1.944	1.971	1.978	2.006	2.009
Ru–N	1.370	1.365	1.384	1.342	1.342	1.326	1.318
Ru–O	–	–	–	–	–	–	–
Ru–Cl	0.553	0.549	0.566	0.582	0.561	0.567	0.557
Ru–N1	0.391	0.394	0.394	0.368	0.372	0.372	0.366
	MS1						
	1	**2**	**2a**	**3**	**4**	**5**	**6**
N–O	1.918	1.920	1.930	1.928	1.943	1.953	1.955
Ru–N	–	–	–	–	–	–	–
Ru–O	0.709	0.703	0.714	0.691	0.699	0.682	0.683
Ru–Cl	0.553	0.551	0.562	0.589	0.576	0.588	0.568
Ru–N1	0.397	0.400	0.384	0.370	0.370	0.365	0.369
	MS2						
	1	**2**	**2a**	**3**	**4**	**5**	**6**
N–O	1.785	1.777	1.791	1.842	1.844	1.824	1.833
Ru–N	0.998	1.000	0.986	0.950	0.952	0.958	0.957
Ru–O	0.557	0.552	0.560	0.543	0.540	0.542	0.546
Ru–Cl	0.601	0.604	0.635	0.635	0.622	0.640	0.619
Ru–N1	0.391	0.394	0.395	0.361	0.361	0.352	0.359

Bonding analysis - Su-Li EDA

The nature of the ruthenium-nitrosyl bonding was evaluated in the light of Su-Li EDA.[92] To assess the total bonding interaction energy in the {Ru–NO}^{6} core, the following fragmentation scheme was adopted. For the complexes [TpRu^{II}Cl$_2$(NO)]^q (Tp = BL(pyrazol-1-yl)$_3$) **1**-**6**, [TpRu^{II}Cl$_2$]$^{q-1}$ and NO$^+$ were considered as interacting fragments, depicted as fragments (f1) and (f2), respectively (Table 2). The fragmentation of complexes **1**-**6** was performed by considering the fragments in the optimized geometry of complexes.

Su-Li EDA shows that the {Ru–NO}^{6} interactions are more covalent than electrostatic since the orbital energy (ΔE^{orb}) has the largest contributions accounting for 71.1-89.2%, while the electrostatic energy (ΔE^{ele}) accounts for 10.5-28.8% (Table 2). The large covalent character of {Ru–NO}^{6} bonds is mainly modulated by polarization term (ΔE^{pol}) which ranges from −188.35 to −306.28 kcal mol^{-1}, while the dispersion component values (ΔE^{disp}) range from −28.15 to –41.09 kcal mol^{-1}. The polarization component (ΔE^{pol}) is related to the orbital stabilization on going from the isolated fragments to the complex orbitals. As previously pointed out, such character is kept mainly by metal-ligand donation and back-donation.[52] It is also important to emphasize that the covalent character observed in all linkage isomers, GS, MS1 and MS2, is larger than the electrostatic and increases on going from **1** to **6**, but such increase is mild. Such small differences (see percentage values depicted in parentheses, Table 2) are consequence of the similarities among the employed pseudoaxial ligands. For instance, compounds **3** and **4** or **5** and **6**, in which the difference observed for the covalent character can be attributed to the coordinating atom, O, N or S and their chemical softness and hardness, which have crucial effect on the donation and back-donation processes. Another issue is the long distance between the pseudoaxial ligands and {Ru–NO}^{6} core. Despite such niceties, the Su-Li EDA

Table 2. Su-Li EDA results (kcal mol^{-1}) for complexes $[TpRu(II)Cl_2(NO)]^q$ (Tp = BL(pyrazol-1-yl)$_3$) **1**-**6**, at M06/def2-SVP level of theory, in which the $[TpRu(II)Cl_2]^{q-1}$ (f1) and NO^+ (f2) were considered as fragments

Su-Li EDA	GS						
	1 q = 0	**2** q = 0	**2a** q = 1	**3** q = 1	**4** q = 1	**5** q = 1	**6** q = 1
ΔE^{ele}	–105.34/*–98.20*[a] (24.6%)[b]	–103.60 (24.2%)	–48.89 (12.6%)	–42.13 (11.9%)	–40.00 (11.2%)	–36.90 (10.5%)	–38.55 (10.8%)
ΔE^{ex}	–50.07/*–46.74*	–50.56	–58.01	–48.64	–48.62	–48.15	–48.48
ΔE^{rep}	226.12/*216.35*	228.42	259.65	222.53	222.12	220.61	222.10
ΔE^{pol}	–292.80/*–284.88*	–293.76	–306.28	–283.09	–286.64	–284.49	–287.68
ΔE^{disp}	–30.46/*–27.96*	–30.16	–31.40	–29.62	–29.55	–29.72	–29.69
ΔE^{orb}	–323.26 (75.4%)	–323.92 (75.8%)	–337.68 (87.4%)	–312.71 (88.1%)	–316.19 (88.8%)	–314.21 (89.5%)	–317.37 (89.2%)
ΔE_{int}^{KS}	–252.55/*–241.43*	–249.66	–184.94	–180.97	–182.69	–178.64	–182.30
q(f1)	–0.201[c]	–0.210	0.710	0.706	0.708	0.704	0.701
q(f2)	0.201	0.210	0.290	0.294	0.292	0.296	0.299
	MS1						
	1	**2**	**2a**	**3**	**4**	**5**	**6**
ΔE^{ele}	–93.20 (28.8%)	–91.21 (28.4%)	–36.92 (13.7%)	–31.63 (12.8%)	–30.30 (12.2%)	–27.16 (11.1%)	–29.03 (11.7%)
ΔE^{ex}	–26.36	–26.83	–31.00	–24.59	–24.20	–23.98	–24.13
ΔE^{rep}	148.73	149.89	168.26	141.91	141.86	140.38	141.71
ΔE^{pol}	–201.28	–201.56	–202.03	–187.41	–190.38	–188.35	–191.15
ΔE^{disp}	–29.13	–28.78	–29.92	–28.26	–28.13	–28.35	–28.15
ΔE^{orb}	–230.41 (71.1%)	–230.34 (71.6%)	–231.95 (86.3%)	–215.67 (87.2%)	–218.51 (87.8%)	–216.70 (88.9%)	–219.30 (88.3%)
ΔE_{int}^{KS}	–201.24	–198.49	–131.60	–130.00	–131.15	–127.46	–130.75
q(f1)	–0.137	–0.147	0.755	0.748	0.743	0.723	0.713
q(f2)	0.137	0.147	0.245	0.252	0.257	0.277	0.287
	MS2						
	1	**2**	**2a**	**3**	**4**	**5**	**6**
ΔE^{ele}	–114.74 (27.4%)	–112.44 (27.0%)	-54.16 (14.8%)	-45.27 (13.5%)	-44.66 (13.2%)	-40.00 (12.0%)	-42.74 (12.6%)
ΔE^{ex}	-41.94	-42.37	-47.02	–38.82	–38.71	–37.98	–38.62
ΔE^{rep}	228.03	229.04	250.72	216.49	216.67	213.43	216.89
ΔE^{pol}	–264.49	–264.84	–269.75	–252.58	–255.17	–253.50	–256.91
ΔE^{disp}	-40.23	–39.23	-41.09	–38.35	–38.73	–38.62	–39.16
ΔE^{orb}	–304.72 (72.6%)	–304.07 (73.0%)	–310.84 (85.2%)	–290.93 (86.5%)	–293.90 (86.8%)	–292.12 (88.0%)	–296.07 (87.4%)
ΔE_{int}^{KS}	–233.38	–229.84	–161.29	–158.53	–160.60	–156.68	–160.53
q(f1)	–0.069	–0.074	0.861	0.850	0.855	0.853	0.852
q(f2)	0.069	0.074	0.139	0.150	0.145	0.147	0.148

[a]Values depicted in italics were obtained with M06/def2-TZVP level of theory. [b]Values in parentheses give the percentage of attractive interactions $\Delta E^{orb} + \Delta E^{ele}$. [c]GAPT (generalized atomic polar tensor) atomic charges for fragments (f1) and (f2).

results are sensitive and precise enough to indicate that the nature of {Ru–NO}^{6} bonds are in fact influenced by the pseudoaxial ligands (Table 2).

The Su-Li EDA results also reveal that the interactions for complexes in GS represent the most stable bonding situation for {Ru–NO}^{6} core, in which the NO group is bound through nitrogen atom, exhibiting ΔE_{int}^{KS} values from –252.55 to –178.64 kcal mol^{-1}. Between the two linkage isomers, MS2 shows {Ru–NO}^{6} bonds more stable than MS1 isomer. According to the ΔE_{int}^{KS} values, the {Ru–NO}^{6} bonds is ca. 30.0 kcal mol^{-1} more stable for MS2 than for MS1 (Table 2, Figure 4). Such evidence, which is in agreement with our previous studies,[52-54] can also be justified by the orbital component of the interaction, ΔE^{orb} (equation 6). Particularly, in the case of ruthenium nitrosyl complexes, {Ru–NO}^{6} bonds have a very strong covalent character, in which the polarization component looks to have the crucial role. The polarization component (ΔE^{pol}) for the {Ru–NO}^{6} core encloses ligand-metal donation and metal-ligand back-donation.

The NO → Ru(II) donation is due to the interaction between the occupied lone-pair orbitals, localized at N (GS) or at O (MS1) atoms and the unoccupied dz^2 orbital of ruthenium(II) ion. On the other hand, the Ru(II) → NO back-donation includes interactions between occupied d orbitals localized on the metal centre and unoccupied doubly degenerated π* (N–O) orbitals. The Su-Li EDA results also reveal that the stabilizing contribution due to dispersion (ΔE^{disp}) is more effective for the MS2 linkage isomer, in which the nitrosyl is bound sideways (η^2) through both nitrogen and oxygen atoms, than for the GS or MS1 linkage isomers. The largest values of dispersion contribution for MS2 justify its relative energy stabilization in comparison with MS1, as pointed above. Large values of Pauli repulsion (equation 7) are observed in cases in which the polarization contribution is also large. It should be emphasized that the repulsion component (ΔE^{rep}) does not vary considerably with the nature of the employed pseudoaxial substituent, but with the kind of linkage isomer (GS, MS1 or MS2).

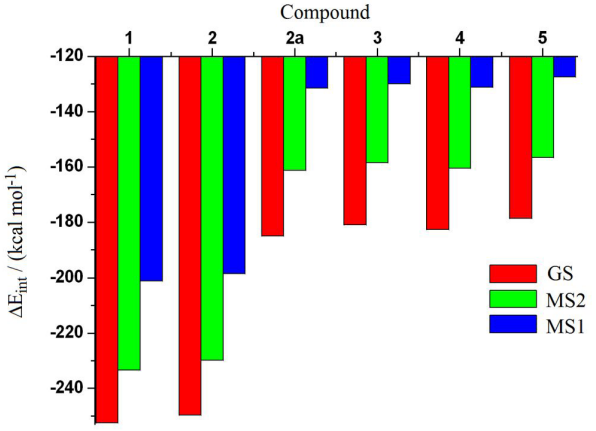

Figure 4. Bond linkage isomerism in the {Ru–NO}^{6} core and total interaction energy, $\Delta E_{int}{}_{KS}$.

The Su-Li EDA results show that the pseudoaxial substituents (Figure 1) have a crucial effect on the lability of {Ru–NO}^{6} bonds, despite the similarities on the bond distance values (Figure 3 and Table S1 in the SI section). For instance, by comparing the total bonding energy ($\Delta E_{int}{}_{KS}$) for complexes **1**-**6** in GS, it is easy to verify that when L = H, **1** and L = pyrazolyl, **2**, the $[TpRu(II)Cl_2]^{q-1}$ interacting fragment acquires negative charge, while NO^+ presents positive charge (close to zero due to the back-donation). This charge configuration is responsible for the largest values of electrostatic component (ΔE^{ele}) observed for **1** and **2**, not only in the GS but also in MS1 and MS2 states. An extensive decrease in the electrostatic term is observed for **2a**-**6**, leading to a considerable decrease in the total bond energy. The results reported in Table 2 also reveal that not only the nature of pseudoaxial substituent, but also the way in which it is bound to boron atom can affect the magnitude of {Ru–NO}^{6} bonds. For instance, by comparing EDA results for complexes **2a**, **4** and **6**, in which all the pseudoaxial substituents (pyrazole, isoxazole and isothiazole, respectively) are bound to boron atom through nitrogen, it is clear that the strongest {Ru–NO}^{6} bonding interaction occurs in **2a**, followed by **4** and **6**. On the other hand, when the pseudoaxial ligands isoxazole and isothiazole are bound to boron by oxygen and sulphur (**3** and **5**), respectively, the magnitude of {Ru–NO}^{6} becomes even more reduced. Finally, two technical points should be emphasized, (*i*) the changes on the EDA components of {Ru–NO}^{6} bonds due to the nature of pseudoaxial ligands are relatively mild, but significant; (*ii*) Su-Li EDA shows to be insensitive to the basis set quality, exhibiting systematic variations in each component, according to the sort of employed basis set.

Conclusions

The Su-Li results shows clearly that the nature of {Ru–NO}^{6} bond in $[TpRu(II)Cl_2(NO)]^q$ (Tp = BL(pyrazol-1-yl)$_3$) **1**-**6** is essentially covalent, which is confirmed by the magnitude of stabilizing components, such as ΔE^{pol} and ΔE^{disp}, but with a reasonable electrostatic character. The results also reveal that not only the nature of pseudoaxial substituent, but also the way in which it is bound to boron atom can affect the magnitude of {Ru–NO}^{6} bonds. In general, {Ru–NO}^{6} bonds become weaker on going from pyrazole to isoxazole and isothiazole as pseudoaxial ligands, respectively, which is attributed to the extensive decrease on the electrostatic component. It was also verified that the magnitude of {Ru–NO}^{6} bonds depends on the metastable state under consideration.

Supplementary Information

Supplementary data (geometrical parameters, vibrational frequencies, electrostatic potential and cartesian coordinates) are available free of charge at http://jbcs.sbq.org.bras as PDF file.

Acknowledgements

Kunitz thanks the scholarship program PIBIC/CNPq-BIP/UFSC for the scholarship granted. Coimbra and Fonseca thank CAPES for MSc and PhD scholarships. Caramori thanks the FAPESC (Grant 17413/2009-0), CNPq (Grant 470985/2011-9) for the financial support and the CENAPAD for the computational resources.

References

1. Nathan, C.; *FASEB J.* **1992**, *6*, 3051.
2. Koshland, D. E.; *Science* **1992**, *258*, 1861.
3. Culotta, E.; Koshland, D. E.; *Science* **1992**, *258*, 1862.
4. Noda, Y.; Mori, A.; Liburdy, R.; Packer, L.; *J. Pineal Res.***1999**, *27*, 159.
5. Rettori, V.; Belova, N.; Dees, W. L.; Nyberg, C. L.; Gimeno, M.; McCann, S. M.; *PNAS* **1993**, *90*, 10130.
6. Whittle, B. J.; *Histochem. J.* **1995**, *27*, 727.
7. Moncada, S.; Palmer, R. M.; Higgs, E. A.; *Pharmacol. Rev.* **1991**, *43*, 109.
8. Ignarro, L. J.; *Nitric Oxide: Biology and Pathobiology*; Academic Press, Orlando, FL, USA, 2000.
9. Bauer, V.; Sotníková, R.; *Gen. Physiol. Biophys.* **2010**, *29*, 319.
10. Ignarro, L. J.; Buga, G. M.; Wood, K. S.; Byrns, R. E.; Chaudhuri, G.; *PNAS* **1987**, *84*, 9265.
11. Furchgott, R. F.; *Angew. Chem., Int. Ed.* **1999**, *38*, 1870.
12. Waldman, S. A.; Murad, F.; *Pharmacol. Rev.* **1987**, *39*, 163.
13. Wink, D. A.; Hines, H. B.; Cheng, R. Y. S.; Switzer, C. H.; Flores-Santana, W.; Vitek, M. P.; Ridnour, L. A.; Colton, C. A.; *J. Leukocyte Biol.* **2011**, *89*, 873.
14. Tfouni, E.; Krieger, M.; McGarvey, B. R.; Franco, D. W.; *Coord. Chem. Rev.* **2003**, *236*, 57, and references therein.
15. Zanichelli, P. G.; Estrela, H. F. G.; Spadari-Bratfisch, R. C.; Grassi-Kassisse, D. M.; Franco, D. W.; *Nitric Oxide* **2007**, *16*, 189.
16. Silva, J. J. N.; Osakabe, A. L.; Pavanelli, W. R.; Silva, J. S.; Franco, D. W.; *Br. J. Pharmacol.* **2007**, *152*, 112.
17. Wink, D. A.; Mitchell, J. B.; *Free Radical Biol. Med.* **1998**, *25*, 434.
18. Ford, P. C.; Lorkovic, I. M.; *Chem. Rev.* **2002**, *102*, 993.
19. Coppens, P.; Novozhilova, I.; Kovalevsky, A.; *Chem. Rev.* **2002**, *102*, 861.
20. Hayton, T. W.; Legzdins, P.; Sharp, W. B.; *Chem. Rev.* **2002**, *102*, 935.
21. Wang, P. G.; Xian, M.; Tang, X.; Wu, X.; Wen, Z.; Cai, T.; Janczuk, A. J.; *Chem. Rev.* **2002**, *102*, 1091.
22. Wyllie, G. R. A.; Scheidt, W. R.; *Chem. Rev.* **2002**, *102*, 1067.
23. Wang, Y.-X.; Legzdins, P.; Poon, J. S.; Pang, C. C. Y.; *J. Cardiovasc. Pharmacol.* **2000**, *35*.
24. Fricker, S. P.; *Platinum Met. Rev.* **1995**, *39*, 150.
25. Fricker, S. P.; Slade, E.; Powell, N. A.; Vaughan, O. J.; Henderson, G. R.; Murrer, B. A.; Megson, I. L.; Bisland, S. K.; Flitney, F. W.; *Br. J. Pharmacol.* **1997**, *122*, 1441.
26. Davies, N. A.; Wilson, M. T.; Slade, E.; Fricker, S. P.; Murrer, B. A.; Powell, N. A.; Henderson, G. R.; *Chem. Commun.* **1997**, 47.
27. Marcondes, F. G.; Ferro, A. A.; Souza-Torsoni, A.; Sumitani, M.; Clarke, M. J.; Franco, D. W.; Tfouni, E.; Krieger, M. H.; *Life Sci.* **2002**, *70*, 2735.
28. Bonaventura, D.; de Lima, R. G.; Vercesi, J. A.; da Silva, R. S.; Bendhack, L. M.; *Vascul. Pharmacol.* **2007**, *46*, 215.
29. Szundi, I.; Rose, M. J.; Sen, I.; Eroy-Reveles, A. A.; Mascharak, P. K.; Einarsdóttir, Ó.; *Photochem. Photobiol.* **2006**, *82*, 1377.
30. Tfouni, E.; Doro, F. G.; Figueiredo, L. E.; Pereira, J. C. M.; Metzker, G.; Franco, D. W.; *Curr. Med. Chem.* **2010**, *17*, 3643.
31. Ostrowski, A. D.; Deakin, S. J.; Azhar, B.; Miller, T. W.; Franco, N.; Cherney, M. M.; Lee, A. J.; Burstyn, J. N.; Fukuto, J. M.; Megson, I. L.; Ford, P. C.; *J. Med. Chem.* **2009**, *53*, 715.
32. Ostrowski, A. D.; Ford, P. C.; *Dalton Trans.* **2009**, 10660.
33. Pereira, A. de C.; Ford, P. C.; da Silva, R. S.; Bendhack, L. M.; *Nitric Oxide* **2011**, *24*, 192.
34. Halpenny, G. M.; Gandhi, K. R.; Mascharak, P. K.; *ACS Med. Chem. Lett.* **2010**, *1*, 180.
35. Von Poelhsitz, G.; Bogado, A. L.; de Araujo, M. P.; Selistre-de-Araújo, H. S.; Ellena, J.; Castellano, E. E.; Batista, A. A.; *Polyhedron* **2007**, *26*, 4707.
36. Ford, P. C.; Bourassa, J.; Miranda, K.; Lee, B.; Lorkovic, I.; Boggs, S.; Kudo, S.; Laverman, L.; *Coord. Chem. Rev.* **1998**, *171*, 185.
37. Olabe, J. A.; *Dalton Trans.* **2008**, 3633.
38. Shaban, S. Y.; van Eldik, R.; *Eur. J. Inorg. Chem.* **2010**, *2010*, 554.
39. McCleverty, J. A.; *Chem. Rev.* **2004**, *104*, 403.
40. Rose, M. J.; Mascharak, P. K.; *Coord. Chem. Rev.* **2008**, *252*, 2093.
41. Silva, J. J. N.; Pavanelli, W. R.; Pereira, J. C. M.; Silva, J. S.; Franco, D. W.; *Antimicrob. Agents Chemother.* **2009**, *53*, 4414.
42. Silva, J. J. N.; Guedes, P. M. M.; Zottis, A.; Balliano, T. L.; Nascimento Silva, F. O.; França Lopes, L. G.; Ellena, J.; Oliva, G.; Andricopulo, A. D.; Franco, D. W.; Silva, J. S.; *Br. J. Pharmacol.* **2010**, *160*, 260.
43. Tfouni, E.; Doro, F. G.; Gomes, A. J.; da Silva, R. S.; Metzker, G.; Benini, P. G. Z.; Franco, D. W.; *Coord. Chem. Rev.* **2010**, *254*, 355.
44. Tfouni, E.; Ferreira, K. Q.; Doro, F. G.; da Silva, R. S.; da Rocha, Z. N.; *Coord. Chem. Rev.* **2005**, *249*, 405.
45. Lang, D. R.; Davis, J. A.; Lopes, L. G. F.; Ferro, A. A.; Vasconcellos, L. C. G.; Franco, D. W.; Tfouni, E.; Wieraszko, A.; Clarke, M. J.; *Inorg. Chem.* **2000**, *39*, 2294.
46. Oliveira, F. de S.; Ferreira, K. Q.; Bonaventura, D.; Bendhack, L. M.; Tedesco, A. C.; Machado, S. de P.; Tfouni, E.; da Silva, R. S.; *J. Inorg. Biochem.* **2007**, *101*, 313.
47. Carlos, R. M.; Ferro, A. A.; Silva, H. A. S.; Gomes, M. G.; Borges, S. S. S.; Ford, P. C.; Tfouni, E.; Franco, D. W.; *Inorg. Chim. Acta* **2004**, *357*, 1381.
48. Toledo Jr., J. C.; Lopes, L. G. F.; Alves, A. A.; Silva, L. P.; Franco, D. W.; *J. Inorg. Biochem.* **2002**, *89*, 267.
49. Benini, P. G. Z.; da Silva, J. J. N.; Osakabe, A. L.; Silva, J. S.; *Nitric Oxide-Biol. Chem.* **2006**, *14*, A53.

50. Venturini, G.; Salvati, L.; Muolo, M.; Colasanti, M.; Gradoni, L.; Ascenzi, P.; *Biochem. Biophys. Res. Commun.* **2000**, *270*, 437.
51. Toledo, J. C.; Silva, H. A. S.; Scarpellini, M.; Miori, V.; Camargo, A. J.; Bertotti, M.; Franco, D. W.; *Eur. J. Inorg. Chem.* **2004**, 1879.
52. Caramori, G. F.; Frenking, G.; *Organometallics* **2007**, *26*, 5815.
53. Caramori, G. F.; Frenking, G.; *Croat. Chem. Acta* **2009**, *82*, 219.
54. Caramori, G. F.; Kunitz, A. G.; Andriani, K. F.; Doro, F. G.; Frenking, G.; Tfouni, E.; *Dalton Trans.* **2012**, *41*, 7327.
55. Kemsley, J.; *Chem. Eng. News* **2007**, *85*, 17.
56. Onishi, M.; *Bull. Chem. Soc. Jpn.* **1991**, *64*, 3039.
57. Trofimenko, S.; *Chem. Rev.* **1993**, *93*, 943, and references therein.
58. Trofimenko, S.; *Scorpionates, the Coordination Chemistry of Polypyrazolylborate Ligands*; Imperial College Press: London, UK, 1999.
59. Trofimenko, S.; *Polyhedron* **2004**, *23*, 197.
60. Arikawa, Y.; Nishimura, Y.; Kawano, H.; Onishi, M.; *Organometallics* **2003**, *22*, 3354.
61. Arikawa, Y.; Asayama, T.; Moriguchi, Y.; Agari, S.; Onishi, M.; *J. Am. Chem. Soc.* **2007**, *129*, 14160.
62. Arikawa, Y.; Ikeda, K.; Asayama, T.; Nishimura, Y.; Onishi, M.; *Chem. Eur. J.* **2007**, *13*, 4024.
63. Arikawa, Y.; Asayama, T.; Tanaka, C.; Tashita, S.; Tsuji, M.; Ikeda, K.; Umakoshi, K.; Onishi, M.; *Organometallics* **2008**, *27*, 1227.
64. Arikawa, Y.; Asayama, T.; Itatani, K.; Onishi, M.; *J. Am. Chem. Soc.* **2008**, *130*, 10508.
65. Onishi, M.; Arikawa, Y.; Yamaguchi, M.; Nagano, T.; Inoue, T.; Terasoba, A.; Matsuo, S.; Nakagawa, M.; Kawano, H.; Nagaoka, J.; Umakoshi, K.; Furukawa, M.; *J. Organomet. Chem.* **2012**, *700*, 135.
66. Fomitchev, D. V.; Novozhilova, I.; Coppens, P.; *Tetrahedron* **2000**, *56*, 6813.
67. Kim, C.; Novozhilova, I.; Goodman, M. S.; Bagley, K. A.; Coppens, P.; *Inorg. Chem.* **2000**, *39*, 5791.
68. Hauser, U.; Oestreich, V.; Rohrweck, H. D.; *Z. Physik A* **1977**, *280*, 17.
69. Hauser, U.; Oestreich, V.; Rohrweck, H. D.; *Z. Physik A* **1977**, *280*, 125.
70. Zöllner, H.; Woike, Th.; Krasser, W; Haussühl, S.; *Z. Kristallogr.* **1989**, *188*, 139.
71. Coppens, P.; *Synchrotron Rad. News* **1997**, *10*, 26.
72. Woike, Th.; Zöllner, H.; Krasser, W.; Haussühl, S.; *Solid State Commun*. **1990**, *73*, 149.
73. Woike, Th.; Haussühl, S.; *Solid State Commun.* **1993**, *86*, 333.
74. da Silva, S. C.; Franco, D. W.; *Spectrochim. Acta, Part A* **1999**, *55*, 1515.
75. Cormary, B.; Malfant, I.; Cointe, M. B. L.; Toupet, L.; Delley, B.; Schaniel, D.; Mockus, N.; Woike, Th.; Fejfarova, K.; Petricek, V.; Dusek, M.; *Acta Crystallogr., Sect. B: Struct. Sci., Cryst. Eng. Mater.* **2009**, *65*, 612.
76. Coppens, P.; Novozhilova, I.; Kovalevsky, A.; *Chem. Rev.* **2002**, *102*, 861.
77. Bitterwolf, T. E.; *Coord. Chem. Rev.* **2006**, *250*, 1196.
78. Netto, A. V. G.; Frem, R. C. G.; Mauro, A. E.; *Quim. Nova* **2008**, *31*, 1208.
79. Chakroborty, S.; Bhanja, C.; Jena, S.; *Heterocycl. Comm.* **2013**, *19*, 79.
80. Hohenberg, P.; Kohn, W.; *Phys. Rev.* **1964**, *136*, B864.
81. Kohn, W.; Sham, L. J.; *Phys. Rev.* **1965**, *10*, A1133.
82. Becke, A. D.; *Phys. Rev. A: At., Mol., Opt. Phys.* **1989**, *38*, 3098
83. Perdew, J. P.; *Phys. Rev. B: Condens. Matter Mater. Phys.* **1986**, *33*, 8822.
84. Schaefer, A.; Horn, H.; Ahlrichs, R.; *J. Chem. Phys.* **1992**, *97*, 2571.
85. Schaefer, A.; Huber, C.; Ahlrichs, R.; *J. Chem. Phys.* **1994**, *100*, 5829.
86. van Lenthe, E.; Baerends, E. J.; Snijders, J. G.; *J. Chem. Phys.* **1993**, *99*, 4597.
87. van Lenthe, E.; Baerends, E. J.; Snijders, J. G.; *J. Chem. Phys.* **1996**, *105*, 6505.
88. van Lenthe, E.; van Leeuwen, R.; Baerends, E. J.; Snijders, J. G.; *Int. J. Quantum Chem.* **1996**, *57*, 281.
89. Neese, F.; *WIREs Comput. Mol. Sci.* **2012**, *2*, 73.
90. Neese, F.; *Coord. Chem. Rev.* **2009**, *253*, 526.
91. Frisch, M. J.; Trucks, G. W.; Schlegel, H. B.; Scuseria, G. E.; Robb, M. A.; Cheeseman, J. R.; Montgomery Jr., J. A.; Vreven, T.; Kudin, K. N.; Burant, J. C.; Millam, J. M.; Iyengar, S. S.; Tomasi, J.; Barone, V.; Mennucci, B.; Cossi, M.; Scalmani, G.; Rega, N.; Petersson, G. A.; Nakatsuji, H.; Hada, M.; Ehara, M.; Toyota, K.; Fukuda, R.; Hasegawa, J.; Ishida, M.; Nakajima, T.; Honda, Y.; Kitao, O.; Nakai, H.; Klene, M.; Li, X.; Knox, J. E.; Hratchian, H. P.; Cross, J. B.; Adamo, C.; Jaramillo, J.; Gomperts, R.; Stratmann, R. E.; Yazyev, O.; Austin, A. J.; Cammi, R.; Pomelli, C.; Ochterski, J. W.; Ayala, P. Y.; Morokuma, K.; Voth, G. A.; Salvador, P.; Dannenberg, J. J.; Zakrzewski, V. G.; Dapprich, S.; Daniels, A. D.; Strain, M. C.; Farkas, O.; Malick, D. K.; Rabuck, A. D.; Raghavachari, K.; Foresman, J. B.; Ortiz, J. V.; Cui, Q.; Baboul, A. G.; Clifford, S.; Cioslowski, J.; Stefanov, B. B.; Liu, G.; Liashenko, A.; Piskorz, P.; Komaromi, I.; Martin, R. L.; Fox, D. J.; Keith, T.; Al-Laham, M. A.; Peng, C. Y.; Nanayakkara, A.; Challacombe, M.; Gill, P. M. W.; Johnson, B.; Chen, W.; Wong, M. W.; Gonzalez, C.; Pople, J. A.; *Gaussian, Inc.*: Wallingford, CT, USA, 2004.
92. Su, P. F.; Li, H.; *J. Chem. Phys.* **2009**, *131*, 014102.
93. Zhao, Y.; Truhlar, D. G.; *Theor. Chem. Acc.* **2008**, *120*, 215.
94. Zhao, Y.; Truhlar, D. G.; *Acc. Chem. Res.* **2008**, *41*, 157.
95. Eichkorn, K.; Weigend, F.; Treutler, O.; Ahlrichs, R.; *Theor. Chem. Acc.* **1997**, *97*, 119.

96. Eichkorn, K.; Öhm, H.; Häser, M.; Ahlrichs, R.; *Chem. Phys. Lett.* **1995**, *242*, 652.
97. Schmidt, M. W.; Baldridge, K. K.; Boatz, J. A.; Elbert, S. T.; Gordon, M. S.; Jensen, J. H.; Koseki, S.; Matsunaga, M.; Nguyen, K. A.; Su, S.; *J. Comput. Chem.* **1993**, *14*, 1347, http://www.msg.ameslab.gov/gamess/index.html, accessed in July 2013.
98. Gordon, M. S.; Schmidt, M. W. In *Theory and Applications of Computational Chemistry, The First Forty Years*; Dykstra, C., ed.; Elsevier: Amsterdam, The Netherlands, 2005.
99. Kitaura, K.; Morokuma, K.; *Int. J. Quantum Chem.* **1976**, *10*, 325.
100. Kitaura, K.; Morokuma, K. In *Molecular Interactions*, vol. 1; Ratajczak, H.; Orville-Thomas, W. J., eds.; John Wiley and Sons: Chichester, UK, 1980, p. 21.
101. Morokuma, K.; Kitaura, K. In *Chemical Applications of Atomic and Molecular Electrostatic Potentials*; Politzer, P.; Truhlar, D. G., eds.; Plenum: New York, USA, 1981; p. 215.
102. Ziegler, T.; Rauk, A.; *Inorg. Chem.* **1979**, *18*, 1755.
103. Hayes, I. C.; Stone, A. J.; *Mol. Phys.* **1984**, *53*, 83.
104. Boys, S. F.; Bernardi, F.; *Mol. Phys.* **1970**, *19*, 553.
105. http://bkchem.zirael.org, accessed in April 30, 2013.
106. http://www.chemcraftprog.com, accessed in April, 2013.
107. Enemark, J. H.; Feltham, R. D.; *Coord. Chem. Rev.* **1974**, *13*, 339.

Submitted: March 24, 2013
Published online: August 16, 2013

J. Braz. Chem. Soc., Vol. 24, No. 9, S1-S9, 2013.
Printed in Brazil - ©2013 Sociedade Brasileira de Química
0103 - 5053 $6.00+0.00

Supplementary Information

The Ru–NO Bonding in Nitrosyl-[poly(1-pyrazolyl)borate]ruthenium Complexes: a Theoretical Insight based on EDA

Giovanni F. Caramori,* André G. Kunitz, Daniel F. Coimbra, Leone C. Garcia and David E. P. Fonseca

Departamento de Química, Centro de Ciências Físicas e Matemáticas, Universidade Federal de Santa Catarina, Campus Universitário Trindade, 88040-900 Florianópolis-SC, Brazil

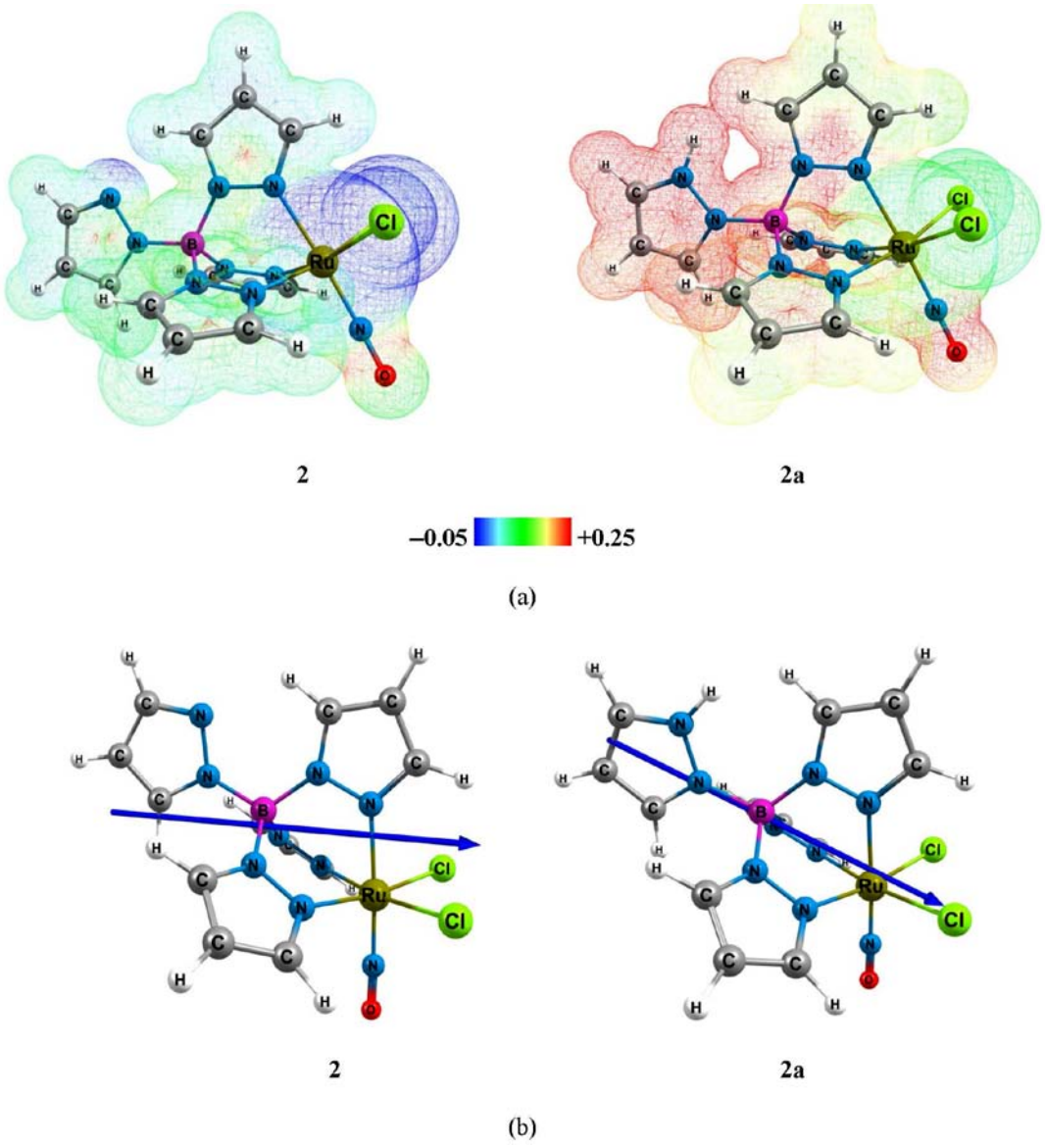

Figure S1. (a) Electrostatic potential surfaces V(r) of complexes **2** and **2a** mapped on electron density isovalue = 0.005 a.u., in which regions of attractive potential appear in blue and those of repulsive potential appear in red. (b) Graphical representation of the dipole moment for complexes **2** (–6.9764, 0.0000, –3.8752, Tot = 7.9805 D) and **2a** (19.136, –0.010, –1.104, Tot = 19.169 D).

*e-mail: giovanni.caramori@ufsc.br

Table S1. Calculated vibrational frequencies, bond lengths *R* (Å), bond angles and relative energies of GS, MS1 and MS2 (eV) for complexes $[TpRuCl_2(NO)]^q$ (Tp = BL(pyrazol-1-yl)$_3$) **1**-**6**, at BP86/TZVP level of theory (experimental values are given in italics)

	GS						
	1	**2**	**2a**	**3**	**4**	**5**	**6**
$\nu(NO^+)$ / cm^{-1}	1880/*1893*[a]	1880/*1894*	1937	1904	1903	1904	1905
ν(BH) / cm^{-1}	2542/*2522*	–	–	–	–	–	–
R(N–O) / Å	1.16	1.16	1.15	1.15	1.15	1.15	1.15
R(Ru–N) / Å	1.75	1.75	1.71	1.76	1.76	1.76	1.76
R(Ru–O) / Å	–	–	–	–	–	–	–
R(Ru-Cl) / Å	2.38	2.38	2.36	2.37	2.37	2.36	2.37
R(Ru–N1) / Å	2.11	2.09	2.06	2.11	2.11	2.11	2.12
R(Ru–N2) / Å	2.11	2.11	2.14	2.14	2.13	2.12	2.13
R(Ru–N3) / Å	2.11	2.09	2.05	2.11	2.10	2.11	2.09
∠Ru–N–O / degree	178.6	178.2	178.9	179.9	179.7	179.7	179.7
∠Ru–O–N / degree	–	–	–	–	–	–	–
ΔE_{rel} / eV	0.00[b]	0.00	0.00	0.00	0.00	0.00	0.00
	MS1						
	1	**2**	**2a**	**3**	**4**	**5**	**6**
$\nu(NO^+)$ / cm^{-1}	1791	1790	1840	1808	1807	1807	1806
ν(BH) / cm^{-1}	2542	–	–	–	–	–	–
R(N–O) / Å	1.16	1.16	1.15	1.15	1.15	1.15	1.15
R(Ru–N) / Å	–	–	–	–	–	–	–
R(Ru–O) / Å	1.86	1.86	1.82	1.87	1.87	1.87	1.87
R(Ru-Cl) / Å	2.37	2.38	2.36	2.36	2.36	2.36	2.37
R(Ru–N1) / Å	2.09	2.08	2.07	2.10	2.10	2.11	2.11
R(Ru–N2) / Å	2.04	2.04	2.05	2.06	2.05	2.04	2.05
R(Ru–N3) / Å	2.09	2.08	2.03	2.10	2.09	2.10	2.08
∠Ru–N–O / degree	–	–	–	–	–	–	–
∠Ru–O–N / degree	178.7	178.5	179.6	178.6	179.2	179.1	179.2
ΔE_{rel} / eV	39.51	39.47	37.06	39.52	39.50	39.22	39.54
	MS2						
	1	**2**	**2a**	**3**	**4**	**5**	**6**
$\nu(NO^+)$ / cm^{-1}	1536	1538	1566	1564	1562	1565	1561
ν(BH) / cm^{-1}	2543	–	–	–	–	–	–
R(N-O) / Å	1.20	1.20	1.20	1.19	1.19	1.19	1.20
R(Ru-N) / Å	1.95	1.95	1.91	1.96	1.96	1.96	1.96
R(Ru-O) / Å	2.21	2.22	2.18	2.22	2.22	2.22	2.22
R(Ru-Cl) / Å	2.35	2.35	2.32	2.33	2.34	2.33	2.34
R(Ru-N1) / Å	2.10	2.09	2.04	2.11	2.11	2.12	2.12
R(Ru-N2) / Å	2.04	2.05	2.02	2.06	2.05	2.05	2.06
R(Ru-N3) / Å	2.14	2.12	2.13	2.14	2.12	2.14	2.12
∠Ru–N–O / degree	86.0	86.2	85.7	86.0	85.9	86.1	85.9
∠Ru–O–N / degree	61.3	61.1	61.1	61.6	61.6	61.5	61.6
ΔE_{rel} / eV	31.94	31.83	30.10	32.54	32.48	32.34	33.66

[a]Experimental values from reference 1. [b]Relative energy values correspond to the ZPE corrected electronic energy differences between each complex in different states.

Table S2. Cartesian coordinates (Å) of optimized structure of **1** in GS

−1.43823454511364	−5.81649533462842	−2.74425252171036	H
2.81220139908169	−6.19539484396843	−3.10496341841030	C
0.46879377461672	−5.09022261461585	−2.53302461988497	C
4.60878846286152	−4.43246946922316	−2.33789529375629	C
6.65916572690751	−4.48626807839201	−2.37662711761820	H
0.84420862923379	−2.79307926180326	−1.51156347237445	N
−4.69580467545762	0.00015873698304	−4.83505291437803	O
3.38797823108983	−2.38456396677023	−1.39406786930857	N
−4.11593469695822	−3.21231686209548	1.78502005100374	Cl
−3.52354339405850	−0.00023999520055	−2.98392079966386	N
−1.68227564900471	−0.00015873698304	−0.22810693435537	Ru
4.40437113349898	0.00023243629660	−0.01792216127568	B
6.67883021554466	0.00038172464969	0.04641167027950	H
0.68827599956022	0.00036093766382	2.97654519913043	N
3.38768910301357	2.38496647840580	−1.39395448574925	N
3.25509458929894	0.00013417054519	2.68354885377924	N
0.84385525047393	2.79289973783434	−1.51202645524165	N
0.18035922780195	−0.00001700753390	5.46542581992220	C
−1.77052585267134	−0.00004346369774	6.09743711789847	H
4.35348648180451	0.00007747876553	4.99746919391843	C
4.60826689848868	4.43338031714965	−2.33699767391171	C
0.46818150339642	5.09031899064126	−2.53278273495843	C
6.65864038308268	4.48759277631000	−2.37534777312393	H
6.39791677816444	0.00009826575141	5.17052841022649	H
−1.43894697181133	5.81627801613973	−2.74417882239680	H
−4.11657531406835	3.21173482649100	1.78466100306591	Cl
2.45564789955662	−0.00021731848869	6.82415959269632	C
2.81147007512411	6.19606947614636	−3.10409792390753	C
2.68680674138355	−0.00048376985308	8.86063792209631	H
3.14734430315616	8.03562512945450	−3.94342539091283	H

Table S3. Cartesian coordinates (Å) of optimized structure of **2** in GS

−1.79433640012744	−8.23498366234562	−3.43790668143407	H
−1.45986434877891	−6.33344877606407	−2.74989335378627	C
2.79285816386260	−5.84312346353348	−2.61864054552353	H
0.87988287644619	−5.14269652586670	−2.37687845117468	C
−5.30570617936751	−4.68072466206876	−1.94075425944852	H
−3.26044440357261	−4.56492036376265	−2.01797602224581	C
−6.49156781870643	−0.00023243629660	−4.06207372683174	H
0.49925426782662	−2.78643498522742	−1.50820164984077	N
5.95121390035421	0.00104501847168	−4.97989852167662	O
−2.04529012168473	−2.41394164698868	−1.29988581576378	N
−11.52738900156307	0.00008125821751	−2.75975016454269	H
−7.37536242794898	−0.00007936849152	−2.20860969024766	C
4.82727291248305	0.00046109314121	−3.09879157333160	N
−9.89726978984314	0.00007180958757	−1.51460971066804	C
5.52553044471494	−3.20136401026568	1.66179290901450	Cl
−5.95535617972117	−0.00006236095762	−0.03093670415903	N
−3.07517944710431	−0.00007747876553	0.08635102904811	B
3.03862836703322	0.00000566917797	−0.30732802724858	Ru
−9.85038379834051	0.00022865684462	1.15811668237460	C
−2.04524854771298	2.41396243397456	−1.29955700344177	N
0.49926560618255	2.78670710576977	−1.50766685738600	N
−7.48923731602074	0.00019842122880	2.05845206319518	N
−11.42904577139143	0.00041573971749	2.47432028204977	H
−3.26053888987204	4.56502996786999	−2.01719934486450	C
−5.30581011429688	4.68069442645294	−1.93998325124518	H
−1.88920253448009	−0.00023621574857	2.77916520934935	N
0.87975059562699	5.14313305257007	−2.37593736763237	C
0.70720916423979	−0.00023054657061	2.92920567339054	N
−1.46007032891166	6.33376625003015	−2.74887101202644	C
2.79269375770159	5.84371683749390	−2.61752749691626	H
−1.79464064601160	8.23537672535124	−3.43662922666579	H
−2.85273602153671	−0.00042140889545	5.16219849806884	C
−4.88899325299603	−0.00035715821184	5.40326706297988	H
1.34418099293607	−0.00053479245477	5.38630866195837	C
5.52562115156239	3.20096905753407	1.66241651859073	Cl
3.32812305012758	−0.00060282259036	5.90533135335151	H
−0.84912380653009	−0.00074077258752	6.86717164592237	C
−0.96801402737554	−0.00102801093779	8.91327246005619	H

Table S4. Cartesian coordinates (Å) of optimized structure of **2a** in GS

−5.89097321529029	−0.02220617009179	−4.98704357563944	O
−4.76662593633159	−0.01347374629857	−3.11862802703372	N
−3.04704520658635	−0.00709214163514	−0.37818708264232	Ru
−5.49350525838650	3.16514741169456	1.57382616424615	Cl
−5.47364801769851	−3.19309456933966	1.57334050466709	Cl
−0.54490815798470	2.74863101682590	−1.49211819195197	N
1.99770115211435	2.41199522922045	−1.21793028936510	N
−0.74648900863839	0.00173287873153	2.94635493673690	N
1.84371494020900	0.02306410569061	2.88128789149815	N
−0.53323910000522	−2.74444905321317	−1.49551969873142	N
2.00537532935396	−2.39012920980660	−1.21429256683709	N
−0.92503598921729	5.11130061829245	−2.31933818454844	C
1.40375082527405	6.34749888878915	−2.60243047599350	C
3.20342759104521	4.59854614800343	−1.85627972830706	C
−0.89604948227848	−5.11192422786869	−2.31649225720964	C
1.44147731491004	−6.33392687673918	−2.58841248861022	C
3.22738553712841	−4.57082008829900	−1.84355809295195	C
−1.48561942427725	0.00380968759298	5.35763207008168	C
0.63732142800417	0.03156220346125	6.94097489440632	C
2.68989077419691	0.04582774494903	5.31807632568875	C
2.93874501018089	0.01401987710927	0.15648442966224	B
−2.84330061967573	5.78143146891033	−2.59834677813218	H
1.72751379944530	8.26334466998221	−3.25238094277934	H
5.24270082518230	4.75803524198751	−1.72729459123062	H
−3.49373107686268	−0.00979256007282	5.77761233268742	H
0.67731747855245	0.04636442712978	8.98909960507391	H
4.67037652255530	0.09603776446557	5.84555365115479	H
−2.80902099024291	−5.79526615287272	−2.59960155618860	H
1.77949071276116	−8.24920196068369	−3.23272590277214	H
5.26769056165527	−4.71521783053829	−1.71270212714682	H
5.88369588050827	0.00501533277369	−0.06620088083190	N
7.16626802676470	0.04724125998848	−2.27532835600043	C
9.75716172559792	0.01981755644223	−1.79161519470388	C
9.98359058327544	−0.04589766481060	0.82889806927433	C
7.63071165215570	−0.05163109345995	1.80028336781349	N
6.12548821047293	0.09631366445990	−4.04152673615793	H
11.27834768270621	0.04250371693512	−3.16356193159015	H
11.62736684471482	−0.09099597552804	2.05598030160212	H
7.08446556817109	−0.12239944200625	3.63682679789584	H

Table S5. Cartesian coordinates (Å) of optimized structure of **3** in GS

1.86456617676698	8.36031217963416	−3.08771022013458	H
1.51254990934049	6.42454490706950	−2.51198252100215	C
−2.73975686358353	5.93155508089502	−2.57712893473242	H
−0.83971864028493	5.20828324575231	−2.29668225967137	C
5.32493603102729	4.79981519386900	−1.63193334866896	H
3.28734465302003	4.63624240202360	−1.80287985132180	C
6.14009390263866	−0.01246085316869	−4.06960806434821	H
−0.50380472800712	2.81062914705919	−1.55051072499906	N
−6.10972222655022	0.00901021351354	−4.94476851554894	O
2.04520508401524	2.42448442827896	−1.27198401154242	N
11.30932596083699	0.00274010268344	−3.07290043756208	H
7.24832181891478	−0.00623987521429	−2.34154624436622	C
−4.90581748347235	0.00622664713237	−3.12672739262077	N
9.73171845488769	0.00146831709313	−1.76135879190075	C
−5.51218142033162	3.18223809353527	1.61245027372672	Cl
5.87661129777709	−0.00596019576798	−0.08520963455101	O
2.85030016473743	−0.00338638897153	0.11090423881772	B
−3.07019434994644	0.00213350064111	−0.36281794117721	Ru
9.84799329496495	0.00770252312945	0.95075138046987	C
2.04158436902113	−2.42794640629004	−1.27583905255912	N
−0.50818511284864	−2.80849753614408	−1.55588321598459	N
7.66127985974696	0.00449754785282	2.08566789688269	N
11.52505707969316	0.01466049421940	2.15166468730782	H
3.27933599428043	−4.64172638684245	−1.80870020736662	C
5.31646816887247	−4.80991577927796	−1.63672758350199	H
1.86584930071323	−0.00511926770306	2.82247017010363	N
−0.84866460311486	−5.20455859582882	−2.30512177593637	C
−0.74635672781919	−0.00275522049135	2.93755637253407	N
1.50115108217738	−6.42543307828413	−2.52087368177841	C
−2.75007098802919	−5.92361823174299	−2.58713881329392	H
1.84940490516061	−8.36122869673862	−3.09879157333160	H
2.80203278353715	−0.01005712171122	5.23197096101915	C
4.81995400372929	−0.01236825659525	5.57016199311320	H
−1.39892068564724	−0.00589594508437	5.38330021818455	C
−5.51722698872113	−3.17788605458357	1.60643338617908	Cl
−3.38802925369152	−0.00473754305337	5.88815941329330	H
0.77906788468149	−0.01051254567446	6.89684601312102	C
0.86836877599778	−0.01365704971946	8.94464002174062	H

Table S6. Cartesian coordinates (Å) of optimized structure of **4** in GS.

−1.90463632725072	−3.35279674315704	8.30479306565956	H
−1.58651178331365	−2.70955652706075	6.38621536807604	C
2.65744064896486	−2.56441184416830	5.88231554716745	H
0.74453060055876	−2.35001800691549	5.17446799569420	C
−5.43168471704270	−1.96887232769147	4.79215391400925	H
−3.39364161704541	−2.03641809249437	4.61672660647586	C
6.02676585024539	−4.81952904970788	0.00000000000000	O
−11.80728985572847	−2.66156876294582	0.00000000000000	H
−6.84530224578873	−3.97814278670926	0.00000000000000	H
0.36231714489298	−1.54934846225787	2.80136246560366	N
−2.19157200955176	−1.37403464410844	2.42463228421976	N
4.78972798583032	−3.02337727486089	0.00000000000000	N
−10.13120154188639	−1.48632212266556	0.00000000000000	C
−7.62148462282059	−2.17521127405838	0.00000000000000	C
5.29761364891936	1.72932341428004	3.18187205361128	Cl
2.89531907483800	−0.30029749634985	0.00000000000000	Ru
−3.11008351570307	−0.00488115277987	0.00000000000000	B
−2.19157200955176	−1.37403464410844	−2.42463228421976	N
0.36231714489298	−1.54934846225787	−2.80136246560366	N
−9.96774918038852	0.99463706535879	0.00000000000000	C
−6.09927604049357	−0.20422194114396	0.00000000000000	N
−3.39364161704541	−2.03641809249437	−4.61672660647586	C
−5.43168471704270	−1.96887232769147	−4.79215391400925	H
0.74453060055876	−2.35001800691549	−5.17446799569420	C
2.65744064896486	−2.56441184416830	−5.88231554716745	H
−11.33417007313555	2.40360436017158	0.00000000000000	H
−1.58651178331365	−2.70955652706075	−6.38621536807604	C
−1.90463632725072	−3.35279674315704	−8.30479306565956	H
−2.10017887409215	2.72782193438554	0.00000000000000	N
0.49666826473865	2.92633119607151	0.00000000000000	N
−7.55239393332271	1.81692149051555	0.00000000000000	O
5.29761364891936	1.72932341428004	−3.18187205361128	Cl
−3.09558809282823	5.10072133883443	0.00000000000000	C
1.08952496179593	5.38214639118017	0.00000000000000	C
−5.11643424980275	5.40903969777431	0.00000000000000	H
3.06366357787237	5.94167431034058	0.00000000000000	H
−1.12561042472179	6.82766185210657	0.00000000000000	C
−1.27092427588473	8.86631718930910	0.00000000000000	H

Table S7. Cartesian coordinates (Å) of optimized structure of **5** in GS

0.40581865604732	8.81245935801749	−2.83360065617636	H
0.32149152353298	6.84257119300305	−2.27292462454296	C
−3.82528917073682	5.78116501754594	−2.30141035409480	H
−1.84222016695204	5.31935378045703	−2.04265584365665	C
4.32250631394775	5.75145474555351	−1.44023954438752	H
2.32480327210741	5.30125020548644	−1.59376655287764	C
7.71622931204285	2.20573730674502	−3.91706938255012	H
−1.18284941611313	2.98537021949710	−1.31149251278564	N
−6.28088226823977	−0.33686633417606	−5.00575375265236	O
1.39884509660770	2.94736027096282	−1.04107839299796	N
11.40810949716396	−1.14869072914357	−3.06377873021521	H
8.04809732097912	1.04703480931396	−2.25133450512344	C
−5.12558505704012	−0.29313996452633	−3.15685340433069	N
9.90965316424630	−0.64320792445860	−1.74396575390187	C
−6.23585009793193	2.44713090452609	1.77140079580405	Cl
6.27380713413853	1.43968963412484	0.56189868434801	S
2.50724308822279	0.53069363909861	0.14843986612886	B
−3.35311656605252	−0.22668775013795	−0.34996024555092	Ru
9.65326081129387	−1.71250559564400	0.76793550888277	C
2.07659532241153	−1.81664839487459	−1.49343344124003	N
−0.40556732249084	−2.56983270269051	−1.68506299483786	N
7.78313128121651	−0.94891267708299	2.20015883562674	N
10.92917923234451	−3.13139690553854	1.56105350628935	H
3.58405808939076	−3.67937586825468	−2.46095991931051	C
5.62305920298550	−3.49886546237365	−2.48287885105204	H
1.47956663193583	0.13706182595163	2.82478886389161	N
−0.42937598022095	−4.85293539140796	−2.78096989766845	C
−1.10685786493440	−0.13217121509319	2.96788836437675	N
2.05463292697226	−5.62020382701676	−3.32518074676336	C
−2.21685267500984	−5.81868930650116	−3.07420245876822	H
2.65000621748196	−7.36528451925188	−4.22082771740627	H
2.46076149808171	0.02832321311682	5.21400722577172	C
4.48276641613517	0.13828069921426	5.54557665800179	H
−1.71431217368908	−0.40220549995716	5.41031763064326	C
−5.35766041597151	−3.84139530533748	1.34781115656013	Cl
−3.68339531543239	−0.65644356528260	5.93063856379056	H
0.48167036750289	−0.30726377656497	6.89794583364637	C
0.60856168818399	−0.47511490804851	8.93676931299819	H

Table S8. Cartesian coordinates (Å) of optimized structure of **6** in GS

−0.66508906168035	−7.83852292939374	−4.69818950965520	H
−0.54364960047630	−6.00802473274886	−3.78346197570561	C
3.62525600566777	−5.08403943118121	−3.54555681209946	H
1.65018243254067	−4.61586359696276	−3.24398111076011	C
−4.52839762958139	−4.97705637378980	−2.79545086791893	H
−2.52169382285745	−4.56108988918380	−2.85948801249390	C
−5.93042502475385	−0.92812947066060	−4.20549637046093	H
1.03300737330074	−2.43679977254653	−2.10282660885899	N
6.52362135092471	1.31809332566374	−4.61775521267733	O
−1.55526527558633	−2.36242771654002	−1.89535359257291	N
−10.89903432337470	−0.19230607550175	−3.79885379388259	H
−6.95458092152408	−0.51224046482013	−2.46770813081573	C
5.27267187936116	0.90025223287708	−2.88028066754623	N
−9.56326828026577	−0.08652110438709	−2.23925537660445	C
5.96976156093211	−3.10606701838763	1.15744582964866	Cl
−5.64616110319588	−0.33749183347828	−0.29775845484242	N
−2.66084946520443	−0.29474056243865	−0.13136430209606	B
3.35690357693363	0.25620338035356	−0.25015436746412	Ru
−10.19840329530116	0.49737210074200	0.22239429269190	C
−1.85529140161504	2.39456628642778	−1.00038314383391	N
0.64911520789889	3.03014916652246	−0.98440551060048	N
−7.60643245265444	0.50327560473032	2.16264588502746	S
−12.05658219822674	0.91366550794401	1.00596350467818	H
−3.23872767251186	4.52211051121739	−1.51396909355791	C
−5.28668230784049	4.48609422360106	−1.59745907745932	H
−1.63523847942299	−0.81605549145595	2.56379502815700	N
0.83603934378517	5.50601713415688	−1.48837086531662	C
0.93161601510952	−0.52771165148863	2.86122845012938	N
−1.58793485847688	6.52534100157431	−1.85872503373629	C
2.68030230453086	6.40610496087295	−1.50979468884914	H
−2.06721850205620	8.46789805961594	−2.30446604101833	H
−2.60050484521114	−1.78162988258023	4.75925978442811	C
−4.58244946203271	−2.26862171846696	4.95297937496931	H
1.52990893227158	−1.23644582460120	5.21784147980254	C
5.49135663993748	3.12267582010125	2.42888937955834	Cl
3.48825654067377	−1.15298040713765	5.82477233445839	H
−0.65291733658792	−2.03282548906406	6.49506948096327	C
−0.79037411527116	−2.71941963249444	8.42141457974887	H

Reference

1. Onishi, M.; *Bull. Chem. Soc. Jpn.* **1991**, *64*, 3039.